Int. J. Electrochem. Sci., 17 **(2022)** Article Number: 220246, doi: 10.20964/2022.02.52

International Journal of
ELECTROCHEMICAL
SCIENCE
www.electrochemsci.org

Short Communication

Influence of Li_2CrO_4 as additive for NaCl electrolyte on Mg-air battery discharge performances

Yanchun Zhao[1,], Cheng Zhang[1,*], Jiankang Wang[1], Hua Zhang[2], Peng Zhang[1], Taiping Xie[1], Songli Liu[1] and Cheng Peng[1]*

[1] Chongqing Key Laboratory of Extraordinary Bond Engineering and Advanced Materials Technology, Yangtze Normal University, Chongqing 408100, China
[2] Institute for Advanced Studies in Precision Materials, Yantai University, Yantai, 264005, China
[*]E-mail: yczhao@yznu.edu.cn (Y. Z.), zhangcheng@cqu.edu.cn (C. Z.)

Received: 14 October 2021 / *Accepted:* 16 December 2021 / *Published:* 5 January 2022

Li_2CrO_4 in different amounts was used as an electrolyte additive for Mg-air batteries based on a 0.6 M NaCl solution in this study. The effect of Li_2CrO_4 content on the corrosion behaviour of AZ31 alloy in 0.6 M NaCl solution was studied by EIS curves, polarization curves and hydrogen evolution tests; the influence of Li2CrO4 content on the discharge performance of Mg-air batteries was studied by constant current discharge tests. The addition of Li_2CrO_4 in different amounts significantly improved the corrosion resistance of the AZ31 alloy and the anode efficiency of the Mg-air battery. The anode efficiency of the Mg-air battery increased obviously with the increase in the added amount of Li_2CrO_4 when this amount was less than 0.02 M but underwent no significant change when it was greater than 0.02 M. In addition, when the added amount of Li2CrO4 reached 0.1 M, the discharge voltage of the battery dropped dramatically, and the voltage lag time also increased greatly. Therefore, the optimal added amount of Li_2CrO_4 is 0.02 M.

Keywords: Mg-air batteries; Corrosion inhibitor; Anodic efficiency; Discharge potential; Electrolyte additive

1. INTRODUCTION

Mg-air batteries are one of the representatives of the new generation of green secondary batteries because of their high energy density, lack of pollution, and abundant material sources [1-3]. However, magnesium is prone to self-corrosion in aqueous electrolyte solution, resulting in the low anode efficiency of Mg-air batteries. Especially in the intermittent discharge process, the hydrogen evolution self-corrosion of the Mg anode during the intermittent discharge period will further reduce the anode efficiency of the battery. Therefore, the intermittent discharge performance of magnesium-air batteries

is extremely poor. Improving the electrolyte can slow down or eliminate the hydrogen evolution self-corrosion of the Mg anode effectively, thereby improving the anode efficiency of Mg-air batteries. At present, two methods are primarily used to improve the electrolyte solution of magnesium-air batteries: replacing the traditional aqueous electrolyte with a nonaqueous electrolyte and adding corrosion inhibitors to the commonly used NaCl electrolyte.

The use of nonaqueous electrolytes in Mg-air batteries can eliminate the hydrogen evolution self-corrosion of the Mg anode. At present, ionic liquids are the most reported nonaqueous electrolytes in Mg-air batteries. Jia et al. [4] incorporated choline nitrate ionic liquid into high polymer chitosan and used it as an electrolyte to prepare a miniature Mg-air battery with a thickness of only 300 μm. The power density of the miniature battery reached 3.9 W L^{-1}, which could drive some miniaturized implanted medical equipment. Zhang et al. [5] found that Mg-air batteries based on the nonaqueous electrolyte 1-ethyl-3-methylimidazolium bis imide have excellent discharge performance, and the addition of water and ethyl acetate can effectively improve the performance of Mg-air batteries. At present, nonaqueous electrolytes have not yet been widely used in Mg-air batteries since they are very expensive. Moreover, the discharge activity of the Mg anode in nonaqueous electrolytes is very poor, which results in a sharp decrease in the power density of Mg-air batteries.

Although using electrolyte additives cannot eliminate the hydrogen evolution self-corrosion of Mg anodes, it can effectively improve the anode efficiency of Mg-air batteries with little or no reduction in the power density of Mg-air batteries. The related research has also been widely reported. Li et al. [6] studied the performance of Mg-air batteries using Na_3PO_4 as an electrolyte additive and found that PO_4^{3-} can react with Mg^{2+} to produce $Mg_3(PO_4)_2$, whose solubility product is much lower than that of $Mg(OH)_2$. $Mg_3(PO_4)_2$ is easily deposited on the surface of the magnesium negative electrode and increases the density of the product film, thereby effectively inhibiting the self-corrosion of the Mg anode and improving the anode efficiency of the battery. Ma et al. [7] studied the influence of Na_2SiO_3 as a Mg-air battery electrolyte additive on its discharge performance and found that Na_2SiO_3 can also effectively improve the anode efficiency of the battery.

We initially studied the influence of Li_2CrO_4 as an electrolyte additive on the intermittent discharge performance of Mg-air batteries and found that the addition of 0.1% Li_2CrO_4 can greatly improve the anode efficiency of Mg-air batteries [8]. However, the addition of Li_2CrO_4 will increase the compactness of the discharge products. Therefore, the addition of excessive Li_2CrO_4 will inevitably reduce the discharge voltage of Mg-air batteries and increase the battery voltage lag time. However, the influence of the content of Li_2CrO_4 on the performance of Mg-air batteries is still not well known, and the optimal added amount of Li_2CrO_4 is not yet clear. Therefore, this paper systematically studies the influence of Li_2CrO_4 content on the discharge performance of Mg-air batteries.

2. EXPERIMENTAL

A rolled AZ31 alloy sheet with a thickness of 2 mm was used as the Mg anode. The mass fraction of its main components is shown as follows: 2.78% Al, 0.94% Zn, 0.33% Mn and balanced Mg. The alloy sheets were cut into small pieces of 20 mm×20 mm and 20 mm×50 mm. The former was used for

electrochemical tests, and the latter was used for discharge tests. Subsequently, the surface of the sample was polished with 1200-grit SiC paper. A 0.6 M NaCl (approximately 3.5% by mass) solution was used as a blank solution, and then Li_2CrO_4 was added to the blank solution in proportion to prepare the other three solutions (0.6 M NaCl + 0.005 M Li_2CrO_4, 0.6 M NaCl + 0.02 M Li_2CrO_4 and 0.6 M NaCl + 0.1 M Li_2CrO_4). In this study, the solutions were prepared with distilled water and superior-grade pure reagents.

The electrochemical tests adopted a standard three-electrode measurement system composed of a working electrode, a reference electrode, and an auxiliary electrode. The reference electrode was a saturated calomel electrode (SCE) with a standard electrode potential of 0.24 V (vs. SHE); the auxiliary electrode was a metal platinum electrode with an area of 15 mm×15 mm; and the working electrode was the AZ31 alloy. Before starting the polarization curve and impedance curve tests, the sample was soaked in the solution for 30 min to make the surface of the sample reach a stable state. The electrochemical tests were completed by a PARSTAT 2273 system at 25±2℃. The polarization curves were scanned at a speed of 1 mV s^{-1}; the EIS curves were measured at open circuit potentials from 100 kHz to 0.01 Hz, and the perturbation amplitude was 5mV. The test area of the working electrode was 1 cm^2.

The Mg-air battery was assembled by an AZ31 alloy anode (the working area of the magnesium negative electrode was 2 cm×3 cm, and the nonworking area was wrapped with AB glue after connecting the wire), a MnO_2 air electrode and NaCl electrolyte containing different contents of Li_2CrO_4. Then, the discharge performance of the battery was studied by a constant current continuous discharge test and constant current intermittent discharge test at 25±2℃ using a battery testing system (BTS-MDTS, China). The discharge current density was 10 mA cm^{-2}. The test time of the continuous discharge test was 4 h; for the intermittent discharge tests, the battery was discharged for 1 h first and then kept in an open circuit for 4 h, and the process was repeated 3 times.

The anode efficiency of the Mg-air battery was calculated by the mass of the consumed Mg anodes. The calculation formula is shown in Eq. 1 [9]:

$$\text{Anodic efficiency } (\%) = \frac{i \times A \times t \times M_a}{2F \times W_c} \times 100\% \qquad (1)$$

where i is the discharge current density, t is the discharge time, F is the Faraday constant (96485), A is the discharge area of the magnesium anode, Ma is the atomic weight of the sample, and Wc is the mass of the consumed Mg anodes.

After 1 h of discharge, the Mg anode was removed, its surface morphology was observed using a scanning electron microscope (SEM) system (TESCAN VEGA-3 LMH), and its corrosion behaviour during the intermittent period of the first discharge cycle was studied through hydrogen evolution test.

3. RESULTS AND DISCUSSION

Figure 1 shows the polarization curve of the AZ31 alloy in the four solutions. The corresponding corrosion parameters are shown in Table 1. The cathode branch of the curve is mainly controlled by the hydrogen evolution reaction, while the anode branch is mainly controlled by the metal dissolution reaction [11, 12]. The addition of Li_2CrO_4 has little effect on the anodic metal dissolution reaction rate

of the alloy, while it greatly reduces the cathodic hydrogen evolution rate of the alloy. And the cathodic hydrogen evolution rate decreases gradually with increasing Li_2CrO_4 content, indicating that the addition of Li_2CrO_4 greatly improves the corrosion resistance of the AZ31 alloy in 0.6 M NaCl solution. The corrosion current density of the alloy in 0.6 M NaCl solution is 196.2×10^{-6} A cm^{-2}, and that in the NaCl solution containing 0.005 M Li_2CrO_4, 0.02 M Li_2CrO_4 and 0.1 M Li_2CrO_4 is only 58.8×10^{-6} Acm^{-2}, 12.6×10^{-6} Acm^{-2} and 10.2×10^{-6} A cm^{-2}, respectively. The corrosion inhibition mechanism of Li_2CrO_4 on magnesium alloys has been widely reported [13-15].

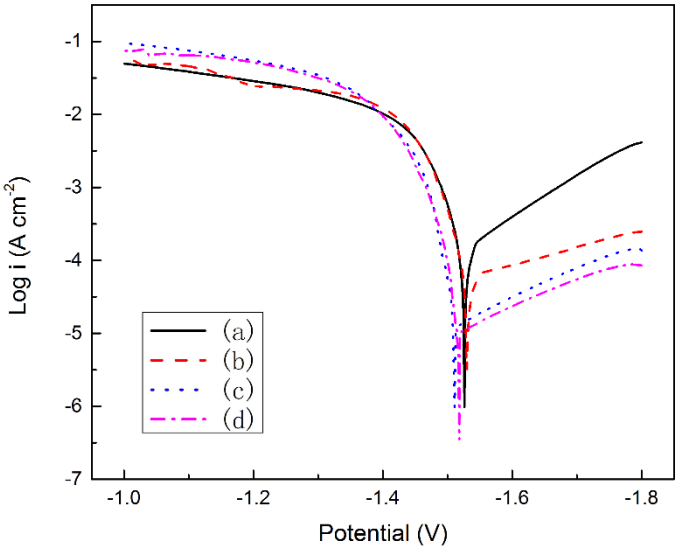

Figure 1. Potentiodynamic polarization curves of the AZ31 Mg alloys in (a) 0.6 M NaCl, (b) 0.6 M NaCl+0.005 M Li_2CrO_4, (c) 0.6 M NaCl+0.02 M Li_2CrO_4 and (d) 0.6 M NaCl+0.1 M Li_2CrO_4.

Table 1. Corrosion parameter of AZ31 Mg alloy in four solutions.

Solutions	Ecorr (V vs. SCE)	Icorr (uA cm^{-2})
0.6 M NaCl	-1.521	196.2
0.6 M NaCl + 0.005 M Li_2CrO_4	-1.520	58.8
0.6 M NaCl + 0.02 M Li_2CrO_4	-1.509	12.6
0.6 M NaCl + 0.1 M Li_2CrO_4	-1.511	10.2

A widely accepted mechanism is that when magnesium alloys are exposed to chromate solution, the surface of magnesium alloys will be oxidized, 5-valent chromium ions will be reduced to trivalent chromium ions, and a dense protective film will be produced and protect the alloy matrix from corrosion.

The chemical composition of the protective film is mainly determined by the oxidation–reduction reaction shown in Eq. 2 and Eq. 3 [13-15]:

$$\mathrm{Mg} + 2\mathrm{Cr}O_4^{2-} + 4H^+ = Mg^{2+} + 2Cr(OH)_3 + 2H_2O \quad (2)$$

$$2\mathrm{Mg} + 2\mathrm{Cr}O_4^{2-} + 10H^+ = 2Mg^{2+} + Cr_2O_3 + 5H_2 \quad (3)$$

In the previous work [16], we also studied the corrosion inhibition mechanism of Li_2CrO_4 on magnesium alloys in NaCl soution. We found that the addition of Li_2CrO_4 produces a dense protective film containing Cr element on the surface of the magnesium alloy, which greatly improves the corrosion resistance of the alloy.

Figure 2 shows the continuous discharge curves of the Mg-air batteries based on the four electrolytes. The addition of Li_2CrO_4 effectively improves the anode efficiency of Mg-air batteries, which increases considerably with increasing Li_2CrO_4 content when the Li_2CrO_4 content is less than 0.02 M but shows little improvement with a further increase to 0.1 M. The anode efficiency of the Mg-air battery with the blank electrolyte is only 62.3%, which increases to 69.1%, 72.2% and 73.0% after the addition of 0.005 M, 0.02 M and 0.1 M Li_2CrO_4, respectively. On the other hand, when the added amount of Li_2CrO_4 is 0.005 M, the discharge voltage of the Mg-air battery is only slightly affected, but when it increases to 0.1 M, the discharge voltage is considerably reduced. The average discharge voltage of the Mg-air battery based on 0.6 M NaCl, 0.6 M NaCl+0.005 M Li_2CrO_4, 0.6 M NaCl+0.005 M Li_2CrO_4, and 0.6 M NaCl+0.005 M Li_2CrO_4 electrolyte is 0.985 V, 0.976 V, 0.964 V and 0.927 V, respectively.

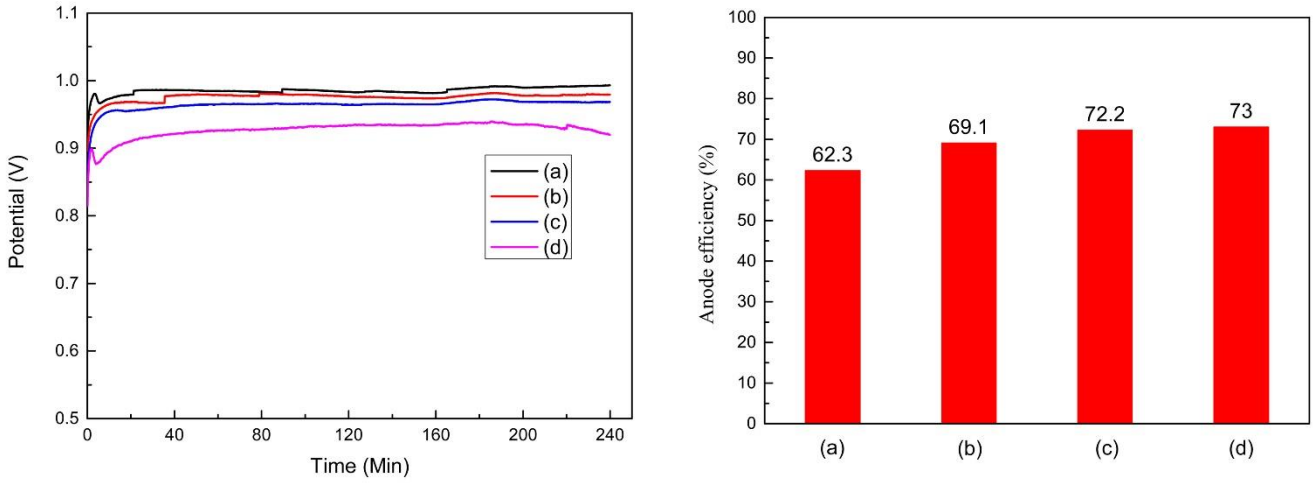

Figure 2. Continuous discharge performance of the Mg-air battery based on (a) 0.6 M NaCl, (b) 0.6 M NaCl+0.005 M Li_2CrO_4, (c) 0.6 M NaCl+0.02 M Li_2CrO_4 and (d) 0.6 M NaCl+0.1 M Li_2CrO_4 electrolyte.

To reveal the influence mechanism of the addition of Li_2CrO_4 on the anode efficiency of Mg-air batteries, the corrosion behaviour of the Mg anode in the corresponding electrolyte after discharge for 1 h was studied through EIS curves, and the results are shown in Figure 3. The Mg anode of the Mg-air

battery based on the blank electrolyte shows a capacitive loop and an inductive loop. It is reported that the capacitive loop in high frequency is caused by the charge transfer process in the double-layer capacitor formed by the alloy surface and the solution interface, while the inductive loop is caused by the chemical reaction in the area which is not covered by the products film.

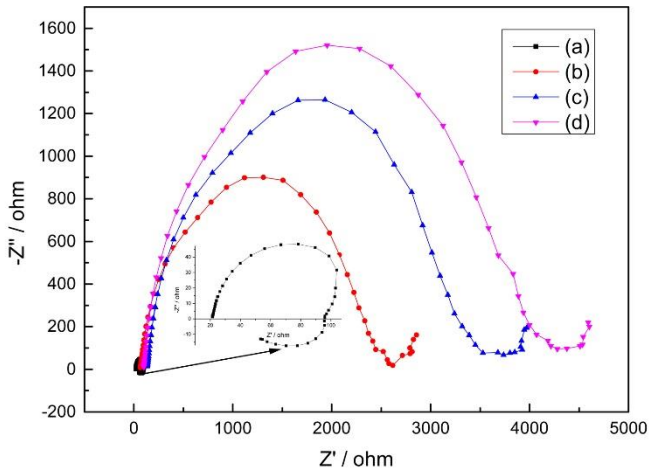

Figure 3. EIS curves of the Mg anodes in (a) 0.6 M NaCl, (b) 0.6 M NaCl+0.005 M Li_2CrO_4, (c) 0.6 M NaCl+0.02 M Li_2CrO_4 and (d) 0.6 M NaCl+0.1 M Li_2CrO_4 electrolyte after discharge for 1 h.

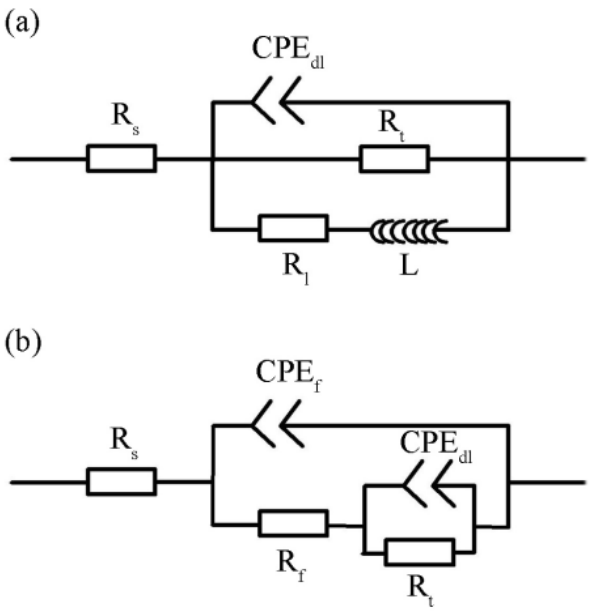

Figure 4. Equivalent circuits of the EIS curve tested in (a) the blank electrolyte and (b) NaCl + Li_2CrO_4 electrolyte.

The existence of the inductive loop indicates the incompleteness of the product film on the alloy surface [17]. However, the anode material of the Mg-air battery based on the Li_2CrO_4 electrolyte shows two capacitive loops. The capacitive loop in the high-frequency region is also caused by the charge transfer process, and the appearance of a capacitive reactance arc in the middle- and low-frequency

regions reflects the presence of a relatively complete protective film on the Mg anode. The EIS curves show that the addition of Li_2CrO_4 produces a relatively complete chromate protective film on the Mg anode surface, which can effectively protect the alloy matrix and slow the self-corrosion rate of the Mg anode.

Table 2. The fitting results of the EIS curves shown in Figure 4

Electrolyte	R_s (Ω cm^2)	Y_{dl} (Ω^{-1} cm^{-2} s^n)	n_{dl}	R_t (Ω cm^2)	Y_f (Ω^{-1} cm^{-2} s^n)	n_f	R_f (Ω cm^2)	L (H cm^2)	R_l (Ω cm^2)
0.6 M NaCl	12.68	207.5	0.85	83.7	-	-	-	63.4	45.9
0.005 M + 0.6 M NaCl	16.1	153.54	0.92	2200	258.3	0.98	124.1	-	-
0.02 M + 0.6 M NaCl	14.7	190.7	0.95	3070	224.3	0.99	200.0	-	-
0.1 M + 0.6 M NaCl	18.5	204.3	0.99	3632	287.5	0.97	176.3	-	-

Fig. 4(a) and Fig. 4(b) show the equivalent circuit of the impedance curve of the Mg anode in the blank electrolyte and the electrolyte containing different levels of Li_2CrO_4. To compensate for the dispersion effect, the long phase angle element CPE is used to replace pure capacitance C. This element mainly includes two parameters, Y and n, where the dimension of Y is Ω^{-1} cm^{-2} s^n, and n is a dimensionless index. Equivalent circuits were achieved based on EIS curve fitting by using ZSimpWin software, and the results are presented in Fig. 4 and Table 2. Among the equivalent circuits, the circuit elements R_s, CPE_{dl}, R_t, CPE_f, R_f, R_l and L represent the solution resistance, capacitive reactance of the electric double layer, charge transfer impedance, film capacitance, film impedance, pitting resistance and inductance, respectively. The charge transfer resistance value R_t equals to the diameters of capacitive loop in high frequency, which reflects the corrosion resistance of the alloy, and a higher R_t value represents a better corrosion performance [18]. In the NaCl solution without Li_2CrO_4, the R_t value of the Mg anode is only 83.7 Ω cm^2. However, the R_t value increases to 2200 Ω cm^2, 3070 Ω cm^2 and 3632 Ω cm^2 after the addition of 0.005 M Li_2CrO_4, 0.02 M Li_2CrO_4 and 0.1 M Li_2CrO_4, respectively, which indicates that the addition of Li_2CrO_4 greatly improves the corrosion resistance of the Mg anode material during the discharge process, thereby increasing the anode efficiency of the Mg-air batteries.

Figure 5 shows the intermittent discharge performance of Mg-air batteries based on the four electrolytes. When the added amount of Li_2CrO_4 was 0.005 M and 0.02 M, the average discharge voltage of the Mg-air battery was close to that without Li_2CrO_4, but when the added amount of Li_2CrO_4 increased to 0.1 M, the average discharge voltage of the battery dropped sharply. The average discharge voltage of the magnesium-air battery based on the blank electrolyte is 0.987 V, and that after the addition of 0.005 M Li_2CrO_4, 0.02 M Li_2CrO_4, and 0.1 M Li_2CrO_4 is 0.977 V, 0.963 V and 0.874 V, respectively. The addition of Li_2CrO_4 substantially improved the anode efficiency of the Mg-air battery. The anode efficiency of the Mg-air battery with the blank electrolyte is only 52.1%, which increases to 66.2% and 71.0% after the addition of 0.005 M Li_2CrO_4 and 0.02 M Li_2CrO_4, respectively. However, when the

added amount of Li_2CrO_4 is further increased to 0.1 M, the anode efficiency of the battery only slightly increases to 71.3%. This result shows that when the added amount of Li_2CrO_4 reaches 0.02 M, further increasing its content will not have a substantial impact on the anode efficiency of the Mg-air battery. Furthermore, the addition of Li_2CrO_4 has a certain impact on the voltage hysteresis of the battery. When the added amount of Li_2CrO_4 is less than 0.02 M, the voltage hysteresis of the battery is not significantly affected. However, when the content of Li_2CrO_4 increases to 0.1 M, the voltage hysteresis of the battery in the third and fourth discharge cycles obviously becomes severe. Continuous discharge and intermittent discharge test results show that the optimal added amount of Li_2CrO_4 is 0.02 M.

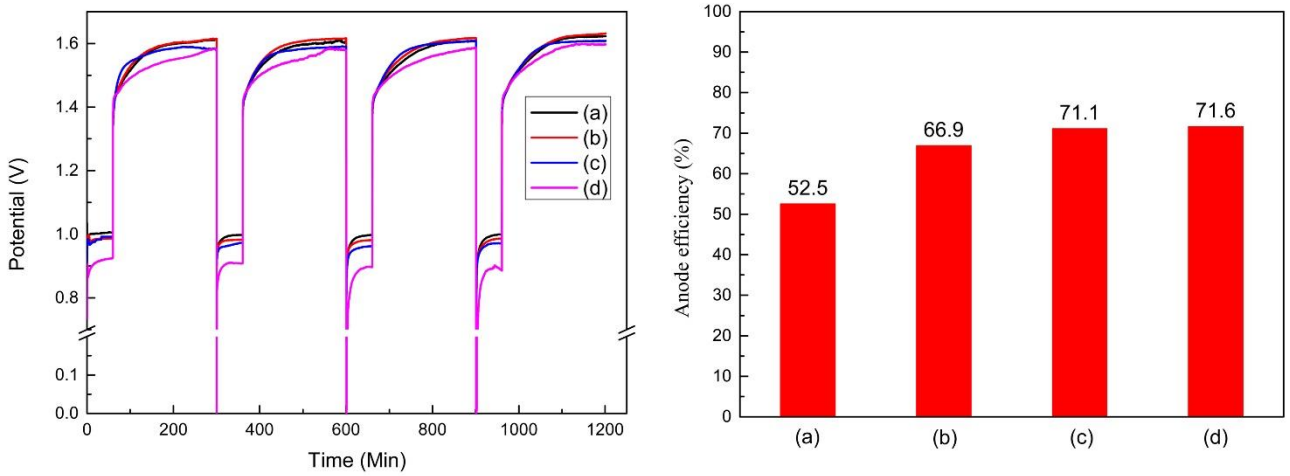

Figure 5. Intermittent discharge performance of the Mg-air battery based on (a) 0.6 M NaCl, (b) 0.6 M NaCl+0.005 M Li_2CrO_4, (c) 0.6 M NaCl+0.02 M Li_2CrO_4 and (d) 0.6 M NaCl+0.1 M Li_2CrO_4 electrolyte.

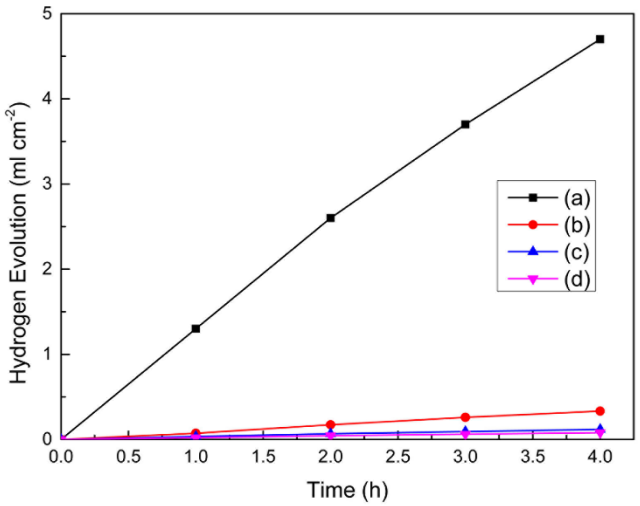

Figure 6. Hydrogen evolution volume–time curves of the Mg anodes in (a) 0.6 M NaCl, (b) 0.6 M NaCl+0.005 M Li_2CrO_4, (c) 0.6 M NaCl+0.02 M Li_2CrO_4 and (d) 0.6 M NaCl+0.1 M electrolyte after discharge for 1 h.

To further understand the influence of Li_2CrO_4 on the self-corrosion behaviour of the Mg anode and the anode efficiency of the Mg-air battery during the intermittent discharge period, the corrosion behaviour of the magnesium anode during the intermittent period of the first discharge cycle was studied through hydrogen evolution tests. The hydrogen evolution volume–time curves of the Mg anodes in the corresponding electrolyte after discharge for 1 h are shown in Fig. 6. The hydrogen evolution rate of the Mg anode is reduced by approximately 20-fold, 45-fold and 55-fold after the addition of 0.005 M Li_2CrO_4, 0.02 M Li_2CrO_4 and 0.1 M Li_2CrO_4, respectively. These results indicate that the addition of Li_2CrO_4 effectively inhibits the self-corrosion hydrogen evolution reaction of the magnesium anode during the discharge interval period and thus effectively improves the anode efficiency of the Mg-air battery. However, when the added amount of Li_2CrO_4 increased from 0.02 M to 0.1 M, the anode efficiency of the battery did not change significantly. This is because when the added amount of Li_2CrO_4 reaches 0.02 M, the self-corrosion rate of the Mg anode during the intermittent period of the discharge test becomes very slow, and the anode efficiency loss of the Mg-air battery during this period can be ignored.

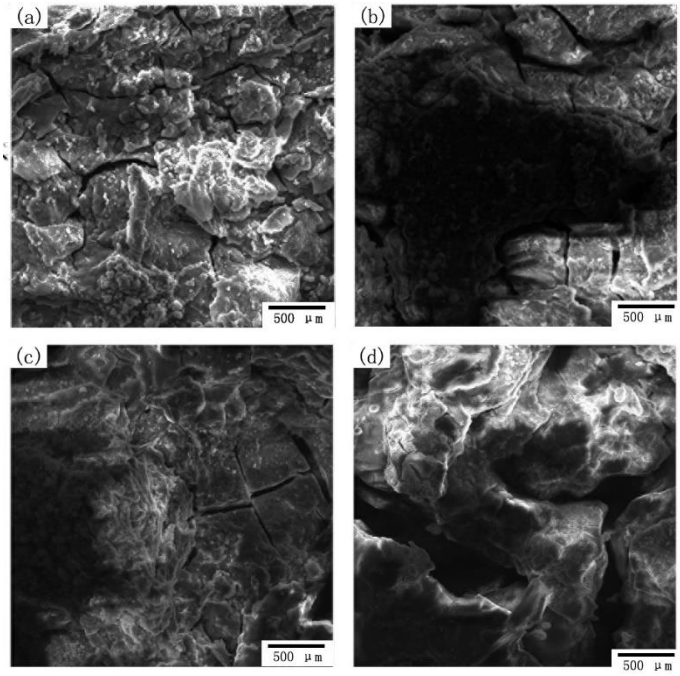

Figure 7. SEM micrographs of the discharge products of the Mg-air battery based on (a) 0.6 M NaCl, (b) 0.6 M NaCl+0.005 M Li_2CrO_4, (c) 0.6 M NaCl+0.02 M Li_2CrO_4, and (d) 0.6 M NaCl+0.1 M Li_2CrO_4 electrolyte at the end of the third discharge cycle.

Figure 7 shows the surface morphology of the discharge products of the Mg-air battery based on the four electrolytes at the end of the third discharge cycle. The morphology of the discharge products film is one of the key factors affecting the performance of the Mg-air battery [19-21]. Cheng et al. [20] found that the addition of Ca element can increase the crack density on the discharge product film of Mg-air battery, thereby reducing the difficulty of the electrolyte passing through the product film and

increasing the battery discharge voltage. Ma et al. [21] used electrolyte additives to reduce the thickness of the product film and increase the crack density on the product film, thereby increasing the discharge voltage of the Mg-air battery. That is, the thin and loose discharge product film can effectively improve the Mg-air battery. In this study, the discharge products of the Mg-air battery based on the blank electrolyte is relatively flat, but lots of cracks can be found. The products film become loose and uneven after the addition of 0.005 M and 0.02M Li_2CrO_4. When the addition amount of Li_2CrO_4 reaches 0.1M, the product film is also very uneven, but the cracks on it almost disappear completely. Therefore, the battery discharge voltage drops sharply, and the voltage hysteresis of the battery also become serious obviously.

4. CONCLUSION

In this paper, Li_2CrO_4 in different amounts was used as an electrolyte additive to improve the discharge performance of Mg-air batteries, and the influence mechanism of the Li_2CrO_4 content on the battery performance was studied. The research results show that the addition of Li_2CrO_4 can effectively improve the corrosion resistance of the Mg anode, thereby increasing the anode efficiency of the Mg-air battery. The anode efficiency of the battery increases considerably with the added amount of Li_2CrO_4 when it is less than 0.02 M but only slightly increases when it is greater than 0.04 M. Moreover, when the added amount of Li_2CrO_4 is less than 0.02 M, the discharge voltage and voltage hysteresis performance of the battery have no obvious changes, but when the added amount of Li_2CrO_4 is further increased to 0.1 M, the discharge voltage of the battery drops substantially, and the voltage hysteresis of the battery also becomes severe. Therefore, the optimal added amount of Li_2CrO_4 is 0.02 M.

ACKNOWLEDGEMENTS
This work is supported by the Science and Technology Research Program of Chongqing Municipal Education Commission (Grant No. KJQN201801419 and KJQN202001440).

References

1. X.J. Gu, W.L. Cheng, S.M. Cheng, H. Yu, Z.F. Wang, H.X. Wang, L.F. Wang, *J. Electrochem. Soc.* 167 (2020) 020501.
2. X. Liu, J.L. Xue, P.J. Zhang, Z.J. Wang, *J. Power Sources.* 414 (2019) 147.
3. S.M. Cheng, W.L. Cheng, X.J. Gu, H. Yu, L.F. Wang, *J Alloy. Compd.* 823 (2020) 153779.
4. X. Jia, Y. Yang, C. Wang, C. Zhao, R. Vijayaraghavan, D.R. Macfarlane, M. Forsyth, G.G. Wallace, *Acs Appl. Mater. Inter.* 6 (2014) 21110.
5. J. Zhang, J. Ma, G. Wang, Y. Li, A.A. Volinsky, *J. Electrochem. Soc.* 166 (2019) A1103.
6. Y. Li, J. Ma, G. Wang, F. Ren, Y. Zhu, Y. Song, *J. Electrochem. Soc.* 165 (2018) A1713.
7. J. Ma, G. Wang, Y. Li, W. Li, F. Ren, *J. Mater. Eng. Perform.* 27 (2018) 2247.
8. Y.C. Zhao, G.S. Huang, G.l. Gong, T.Z. Han, D.B. Xia, F.S. Pan, *Acta. Metall. Sin-Engl.* 29 (216) 1019.

9. X. Chen, Q. Liao, Q. Le, Q. Zou, H. Wang, A. Atrens, *Electrochim. Acta.* 348 (2020) 136315.
10. Y.C. Zhao, G.S. Huang, G.G. Wang, T.Z. Han, F.S. Pan, *Acta. Metall. Sin-Engl.* 28 (2015) 1387.
11. N. Wang, W. Li, Y. Huang, G. Wu, M. Hu, G. Li, Z. Shi, *J. Power Sources.* 436 (2019) 226855.
12. T. Zheng, Y. Hu, Y. Zhang, S. Yang, F. Pan, *Mater. Design.* 137 (2018) 245.
13. M. Bethencourt, F. Botana, J. Calvino, M. Marcos, M. Rodriguez-Chacon, *Corros. Sci.* 40 (1998) 1803.
14. S. Pommiers, J. Frayret, A. Castetbon, M. Potin-Gautier, *Corros. Sci.* 84 (2014) 135.
15. K. Yang, M. Ger, W. Hwu, Y. Sung, Y. Liu, *Mater. Chem. and Phys.* 101 (2007) 480.
16. Y.C. Zhao，G.S. Huang，G.L. Gong，T.Z. Han，D. B. Xia，F. S. Pan, *Acta. Metall. Sin-Engl.*, 29 (2016) 1019
17. X. Chen，Q. Zou，Q. Le，J. Hou，A. Atrens. *J. Power Sources.* 451(2020) 227807
18. S.M. Cheng，W.L. Cheng，X.J. Gu，H. Yu，L.F. Wang, *J. Alloy. Compd.* 823 (2020) 153779
19. F.E.T. Heakal, A.M. Fekry, M.Z. Fatayerji, *J. appl. Electrochem.* 39 (2009) 1633.
20. S.M. Cheng, W.L. Cheng, X.J. Gu, H. Yu, Z. F. Wang, H. X. Wang, L. F Wang. *J. Alloy. Compd.* 823 (2020) 153779.
21. J. Ma, G. Wang, Y. Li, W. Li, F. Ren. *J. Mater. Eng. Perform.*, 27 (2018) 2247.